Main-Group Multiple Bonding

International Edition: DOI: 10.1002/anie.201705209
German Edition: DOI: 10.1002/ange.201705209

Bismuth–Boron Multiple Bonding in BiB_2O^- and Bi_2B^-

*Tian Jian, Ling Fung Cheung, Teng-Teng Chen, and Lai-Sheng Wang**

Abstract: *Despite its electron deficiency, boron is versatile in forming multiple bonds. Transition-metal–boron double bonding is known, but boron–metal triple bonds have been elusive. Two bismuth boron cluster anions, BiB_2O^- and Bi_2B^-, containing triple and double B–Bi bonds are presented. The BiB_2O^- and Bi_2B^- clusters are produced by laser vaporization of a mixed B/Bi target and characterized by photoelectron spectroscopy and ab initio calculations. Well-resolved photoelectron spectra are obtained and interpreted with the help of ab initio calculations, which show that both species are linear. Chemical bonding analyses reveal that Bi forms triple and double bonds with boron in BiB_2O^- ($[Bi{\equiv}B{-}B{\equiv}O]^-$) and Bi_2B^- ($[Bi{=}B{=}Bi]^-$), respectively. The Bi–B double and triple bond strengths are calculated to be 3.21 and 4.70 eV, respectively. This is the first experimental observation of Bi–B double and triple bonds, opening the door to design main-group metal–boron complexes with multiple bonding.*

To compensate for its electron deficiency, boron tends to form delocalized bonds in its compounds[1] and at the nanoscale.[2] Despite the fact that boron has only three valence electrons, it is capable of forming B–B triple bonds, as well as multiple bonds with various elements. The first B–B triple bond was observed in 2002 by Zhou et al. in OCBBCO, which was formed in a low temperature argon matrix and characterized by infrared spectroscopy and theoretical calculations.[3] In 2007, Li et al. studied the $B_4O_2^-$ ($[OBBBBO]^-$) boron oxide cluster using photoelectron spectroscopy (PES) and ab initio calculations, and found it to be linear with a 2.5-fold B–B bond, whereas a B≡B triple bond is formed in the closed-shell $[OBBBBO]^{2-}$ species.[4] The nature of the B≡B triple bonds in these species was further studied and confirmed by more sophisticated theoretical analyses.[5] The first chemical compound containing a B≡B triple bond was synthesized in 2012 by Braunschweig et al. and confirmed by X-ray crystallography and density functional theory (DFT) studies.[6] Unlike the long-sought B≡B triple bond, boron readily forms a triple bond with O in the gaseous BO^- species,[7] which is isoelectronic to the well-known CN^- and CO species. Neutral boronyl (•BO) can be viewed as a σ radical and has been found in a wide variety of gaseous clusters,[4,8] including boronyl metal complexes.[9,10] Even though CN^- and CO are common ligands in a vast number of chemical compounds, the first chemical compound with a boronyl unit was synthesized and crystallized only in 2010.[11]

Metal atoms can also form multiple bonds with boron. Using PES and ab initio calculations, the structures and bonding of many transition metal doped boron clusters have been characterized.[12] However, multiple M–B bonds have not been observed in these boron-rich clusters; the transition metal atoms in these clusters interact with neighboring boron atoms mainly through delocalized bonds. Using matrix isolation infrared spectroscopy and theoretical calculations, Andrews and co-workers characterized three transition-metal fluoride complexes $FBMF_2$ (M = Ti, Zr, Hf) and found them to possess an M=B double bond.[13] In condensed phase, although transition-metal complexes of boron usually feature two-center two-electron (2c–2e) bonds, a number of transitional-metal terminal borylene complexes were characterized to have an M=B double bond, which have been extensively reviewed.[14]

However, to the best of our knowledge, there has been no observation of metal–boron triple bonds, although a previous B=Pt compound stabilized by a transition-metal base was inferred to exhibit possible partial triple-bond character via an electron localization function analysis.[15] There have also been very few studies about multiple bonding between boron and main-group metal elements. There is only one recent computational study, which considered a Bi–B triple bond stabilized by bulky ligands as RB≡BiR.[16] A recent PES and theoretical study on the $BiBO^-$ species showed that it contains a Bi–B single bond and a B≡O triple bond,[10] which is confirmed subsequently by a high-level ab initio calculation.[17] In the current article, we report the first observation of Bi≡B triple bonding and Bi=B double bonding in two clusters, BiB_2O^- ($[Bi{\equiv}B{-}B{\equiv}O]^-$) and Bi_2B^- ($[Bi{=}B{=}Bi]^-$) using a joint PES and theoretical study.

The experiment was carried out using a magnetic-bottle PES apparatus equipped with a laser vaporization supersonic cluster source, details of which have been published elsewhere.[2a,18] The BiB_2O^- and Bi_2B^- cluster anions were produced by laser vaporization of a Bi/^{11}B mixed target, which was used to produce small bare boron clusters (B_n^-).[2a] The BiB_2O^- and Bi_2B^- clusters were observed to be particularly prominent in the mass spectra, indicating their unusual thermodynamic stability. The BiB_2O^- species was produced due to trace amount of oxide impurity on the target surface. Clusters formed in the nozzle were entrained by a He carrier gas seeded with 5% Ar and cooled by a supersonic expansion. Negatively charged species were extracted from the collimated cluster beam after a skimmer and analyzed by a time-of-flight mass spectrometer. The BiB_2O^- and Bi_2B^- clusters of current interest were each mass-selected and photodetached by a pulsed laser beam. Three detachment photon energies were used in the current experiment: 193 nm

[*] T. Jian, L. F. Cheung, T. T. Chen, Prof. Dr. L. S. Wang
Department of Chemistry, Brown University
Providence, RI 02912 (USA)
E-mail: Lai-Sheng_Wang@brown.edu

Supporting information and the ORCID identification number(s) for the author(s) of this article can be found under: https://doi.org/10.1002/anie.201705209.

(6.424 eV) from an ArF excimer laser, and 266 nm (4.661 eV) and 355 nm (3.496 eV) from an Nd:YAG laser. The photoelectron spectra were calibrated by the known spectra of Bi^-. The resolution of the PES apparatus was $\Delta E_k/E_k \approx 2.5\,\%$, that is, about 25 meV for 1 eV kinetic energy electrons. The PE spectra of BiB_2O^- and Bi_2B^- are shown in Figures 1 and 2, respectively.

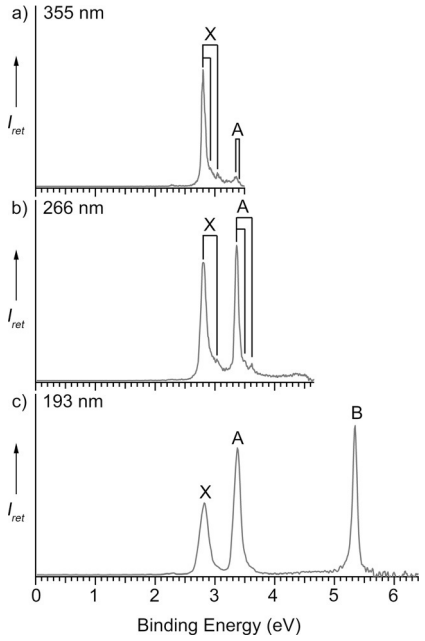

Figure 1. Photoelectron spectra of BiB_2O^- at a) 355 nm (3.496 eV), b) 266 nm (4.661 eV), and c) 193 nm (6.424 eV). The resolved vibrational structures are labeled for bands X and A in (a) and (b).

The 355 nm spectrum of BiB_2O^- (Figure 1 a) exhibits an intense ground-state band X, which displays two short vibrational progressions with frequencies of 1010 cm^{-1} and 1935 cm^{-1}, respectively. The sharp 0–0 transition at 2.80 eV defines the first vertical detachment energy (VDE) and adiabatic detachment energy (ADE) of BiB_2O^-, which is also the electron affinity (EA) of neutral BiB_2O. The 355 nm spectrum also shows a weak band A near threshold at 3.36 eV, with a short 300 cm^{-1} vibrational progression. The band A was clearly cut off in the 355 nm spectrum, because the 266 nm spectrum (Figure 1 b) shows that band A has similar intensity as band X, also with two similar high-frequency vibrational progressions at 1010 cm^{-1} and 1935 cm^{-1}. Bands X and A have similar intensities and the same vibrational features, suggesting that they may have the same electronic origin. Following a large energy gap from band A, another sharp band B is observed at a VDE of 5.35 eV in the 193 nm spectrum (Figure 1 c). The short vibrational progressions and sharp PES bands observed for BiB_2O^- suggest that there is little geometry change from the anion ground state to the neutral states. The 355 nm spectrum of Bi_2B^- (Figure 2 a) displays three sharp and closely-spaced bands (X, A, B) at VDEs of 2.62, 2.76, and 3.02 eV. Since no vibrational features are resolved for band X, the first ADE is estimated from the onset of band X to be 2.55 eV, which also represents the EA of

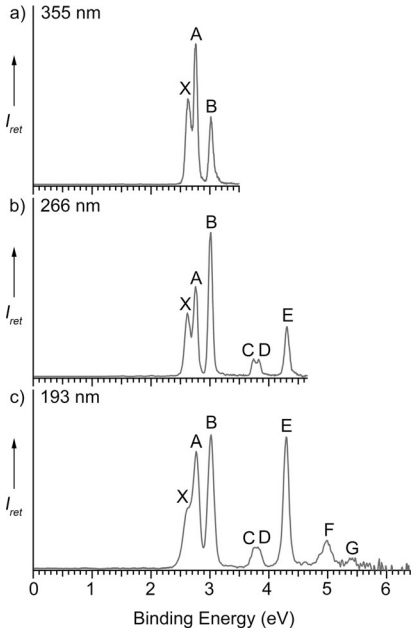

Figure 2. Photoelectron spectra of Bi_2B^- at a) 355 nm, b) 266 nm, and c) 193 nm.

neutral Bi_2B. The 266 nm spectrum (Figure 2 b) shows three more bands C, D, and E. The weak bands C and D at VDEs of 3.74 eV and 3.83 eV are closely spaced. The band E at a VDE of 4.30 eV becomes significantly more intense at 193 nm (Figure 2 c), which shows a weak and broad band F at 4.99 eV, as well as a very weak band G at 5.42 eV. The observed spectroscopic constants for both BiB_2O^- and Bi_2B^- are summarized in Table 1, where they are compared with the theoretical data.

To understand the observed PE spectra, the structures and bonding of BiB_2O^- and Bi_2B^-, we performed ab initio calculations at different levels of theory. Several initial structures were optimized using the PBE0 and CCSD methods with different spin multiplicities.[19] The lowest energy structures of BiB_2O^- and Bi_2B^- were both found to be linear with a singlet ground state and a triplet ground state, respectively. For BiB_2O^- ($^1\Sigma^+$), the first VDE (VDE_1) was calculated as the energy difference between the anion ground state and the neutral ground state at the anion geometry. For Bi_2B^- ($^3\Sigma_g^-$), the first two VDEs were calculated as the energy differences between the anion triplet ground state and the lowest neutral doublet and quartet states at the anion geometry, respectively. To compute the energies of the neutral excited states, we used the complete active space self-consistent field (CASSCF) method.[20] We chose an active space with 15 electrons and 8 orbitals for BiB_2O and 13 electrons and 10 orbitals for Bi_2B. The state-averaged (SA)-CASSCF method was employed to study the low-lying electronic states of the neutral species simultaneously. The $^2\Pi$ and $^2\Sigma^+$ states were included in the SA3-CASSCF(15,8) calculations of BiB_2O. For Bi_2B, we performed two separate CASSCF calculations. While the $^2\Pi_g$ ground state was calculated alone at the SA2-CASSCF(13,10) level, the $^4\Pi_u$, $^2\Pi_u$, $^4\Sigma_u^-$, $^2\Sigma_u^-$, $^4\Sigma_g^-$, and $^2\Sigma_g^-$ excited states were included in

Table 1: All of the observed VDEs, term values, their assignments, and comparison with theoretical results for BiB_2O^- and Bi_2B^-. All energies are in eV.

	VDE (expt.)	Term value	Spin-free states	State	Composition of SO coupled state	MRCI ΔE [eV]
BiB_2O^- ($C_{\infty v}$, $^1\Sigma^+$)						
X	2.80(2)	0	$^2\Pi$ ($1\sigma^2 2\sigma^2 3\sigma^2 4\sigma^2 1\pi^4 5\sigma^2 2\pi^3$)	$^2\Pi_{3/2}$	$100\%\,^2\Pi$	0
A	3.36(3)	0.56(3)		$^2\Pi_{1/2}$	$94.2\%\,^2\Pi + 5.8\%\,^2\Sigma^+$	0.54
B	5.35(3)	2.55(3)	$^2\Sigma^+$ ($1\sigma^2 2\sigma^2 3\sigma^2 4\sigma^2 1\pi^4 5\sigma^1 2\pi^4$)	$^2\Sigma^+_{1/2}$	$94.2\%\,^2\Sigma^+ + 5.8\%\,^2\Pi$	2.74
Bi_2B^- ($D_{\infty h}$, $^3\Sigma_g^-$)						
X	2.62(2)	0	$^2\Pi_g$ ($1\sigma_g^2 1\sigma_u^2 2\sigma_g^2 2\sigma_u^2 1\pi_u^4 1\pi_g^1$)	$^2\Pi_{g,1/2}$	$100\%\,^2\Pi_g$	0[a]
				$^2\Pi_{g,3/2}$	$100\%\,^2\Pi_g$	1.02[a]
A	2.76(2)	0[b]		$^4\Pi_{u,3/2}$	$69.6\%\,^4\Pi_u + 29.9\%\,^2\Pi_u + 0.5\%\,^4\Sigma_u^-$	0
B	3.02(2)	0.26(2)	$^4\Pi_u$ ($1\sigma_g^2 1\sigma_u^2 2\sigma_g^2 2\sigma_u^2 1\pi_u^3 1\pi_g^2$)	$^4\Pi_{u,1/2}$	$74.9\%\,^4\Pi_u + 19.5\%\,^2\Pi_u + 4.9\%\,^4\Sigma_u^- + 0.8\%\,^2\Sigma_u^-$	0.14
				$^4\Pi_{u,5/2}$	$100\%\,^4\Pi_u$	0.15
				$^4\Pi_{u,-1/2}$	$80.3\%\,^4\Pi_u + 9.7\%\,^2\Sigma_u^- + 9.4\%\,^4\Sigma_u^- + 0.6\%\,^2\Pi_u$	0.38
C	3.74(3)	0.98(3)	$^2\Pi_u$ ($1\sigma_g^2 1\sigma_u^2 2\sigma_g^2 2\sigma_u^2 1\pi_u^3 1\pi_g^2$)	$^2\Pi_{u,3/2}$	$49.9\%\,^2\Pi_u + 32.8\%\,^4\Sigma_u^- + 17.3\%\,^4\Pi_u$	0.64
D	3.83(3)	1.07(3)		$^2\Pi_{u,1/2}$	$60.3\%\,^2\Pi_u + 24.4\%\,^4\Sigma_u^- + 7.64\%\,^4\Pi_u + 7.61\%\,^2\Sigma_u^-$	0.86
E	4.30(3)	1.54(3)	$^4\Sigma_u^-$ ($1\sigma_g^2 1\sigma_u^2 2\sigma_g^2 2\sigma_u^1 1\pi_u^4 1\pi_g^2$)	$^4\Sigma_{u,3/2}^-$	$66.7\%\,^4\Sigma_u^- + 20.1\%\,^2\Pi_u + 13.2\%\,^4\Pi_u$	1.55
				$^4\Sigma_{u,1/2}^-$	$61.2\%\,^4\Sigma_u^- + 22.6\%\,^4\Pi_u + 14.6\%\,^2\Pi_u + 1.6\%\,^2\Sigma_u^-$	1.62
F	4.99(4)	2.23(4)	$^2\Sigma_u^-$ ($1\sigma_g^2 1\sigma_u^2 2\sigma_g^2 2\sigma_u^1 1\pi_u^4 1\pi_g^2$)	$^2\Sigma_{u,1/2}^-$	$80.3\%\,^2\Sigma_u^- + 14.5\%\,^4\Pi_u + 5\%\,^2\Pi_u$	1.97
G	5.42(5)	2.66(5)	$^2\Sigma_g^-$ ($1\sigma_g^2 1\sigma_u^2 2\sigma_g^1 2\sigma_u^2 1\pi_u^4 1\pi_g^2$)	$^2\Sigma_{g,1/2}^-$	$100\%\,^2\Sigma_g^-$	2.59

[a] These first two ΔE of Bi_2B are with respect to the $^2\Pi_g$ ground state, while the others are with respect to $^4\Pi_u$. [b] The term values of band B–G in Bi_2B^- are with respect to band A to facilitate comparison with the theoretical data.

the SA8-CASSCF(13,10) calculations, both followed by multi-reference configuration interaction (MRCI) calculations to account for the dynamic electron correlation effect.[21] As shown previously for BiBO,[17] spin–orbit (SO) coupling is expected to be important for BiB_2O and Bi_2B, as well. We carried out the SO coupling calculations using the state-interaction method based on the MRCI wavefunctions (MRCI + SO).[22] For all the calculations, we employed the aug-cc-pVTZ-pp basis set with the relativistic effective core potential (ECP60MDF) for Bi[23] and the aug-cc-pVTZ basis set for B and O[24] (hereafter denoted as AVTZ). All of the DFT calculations were performed using Gaussian 09.[25] The CCSD, CASSCF, and MRCI calculations were performed using Molpro2012.[26]

The optimized structures of BiB_2O^- and Bi_2B^- at the PBE0/AVTZ and CCSD/AVTZ levels are shown in Figure 3. The two levels of theory give almost identical bond lengths. The linear BiB_2O^- ($C_{\infty v}$, $^1\Sigma^+$) and Bi_2B^- ($D_{\infty h}$, $^3\Sigma_g^-$) structures are significantly more stable than any bent or cyclic arrangements. The molecular orbital (MO) pictures for BiB_2O^- and Bi_2B^- are given in the Supporting Information, Figure S1. The calculated VDE_1 for the linear BiB_2O^- and Bi_2B^- (both doublet and quartet final states) are compared with the experimental values in Table 2. The calculated VDE_1 for BiB_2O^-, derived from electron detachment from the 2π HOMO, is slightly overestimated at both levels of theory compared to the experimental value of 2.80 eV. We also computed the vibrational frequencies for the neutral ground state of BiB_2O at the PBE0/AVTZ level. The three observed frequencies, 1935, 1010, and 300 cm^{-1} are in excellent agreement with the calculated frequencies for the B–O, B–B, and Bi–B stretching vibrations, respectively. For Bi_2B^-, the calculated VDE_1 to the $^2\Pi_g$ neutral ground state at the PBE0/AVTZ and CCSD/AVTZ levels is 2.58 eV and 2.60 eV, respectively, both agreeing well with the experimental VDE_1 at 2.62 eV. The calculated VDE from the lowest $^4\Pi_u$ quartet state at the PBE0/AVTZ level (2.77 eV) is in perfect agreement with the experimental VDE at 2.76 eV, while CCSD seems to underestimate the VDE by 0.08 eV.

Table 2: The experimental first vertical detachment energies (VDE) for BiB_2O^- and Bi_2B^- in comparison with the calculated VDEs at PBE0/AVTZ and CCSD/AVTZ levels.

	Transition	VDE [eV]			Frequency [cm^{-1}]	
		Expt.	PBE0	CCSD	Expt.	PBE0[a]
BiB_2O^-	$^1\Sigma^+ \rightarrow {}^2\Pi$	2.80	2.96	2.95	1935, 1010, 300	1991, 1043, 321
Bi_2B^-[b]	$^3\Sigma_g^- \rightarrow {}^2\Pi_g$	2.62	2.58	2.60	–	–
	$^3\Sigma_g^- \rightarrow {}^4\Pi_u$	2.76	2.77	2.68	–	–

[a] Vibrational frequencies were calculated at the PBE0/AVTZ level. The listed frequencies are for the B–O (1991 cm^{-1}), B–B (1043 cm^{-1}), and Bi–B (321 cm^{-1}) stretching modes. [b] The first and second VDEs represent the transitions to the lowest doublet and quartet states of neutral Bi_2B, respectively.

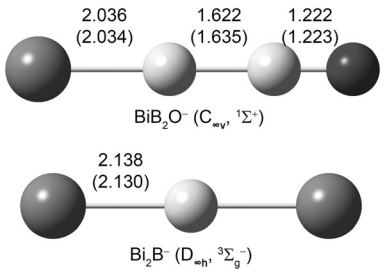

Figure 3. The optimized structures of BiB_2O^- and Bi_2B^- at the PBE0/AVTZ and CCSD/AVTZ levels of theory. Bond lengths are given in Å and the values in parentheses are from the CCSD/AVTZ level.

The higher binding energy PES bands correspond to detachment transitions to excited states of the neutral species. To understand these detachment transitions, we calculated the ΔE (or the term values) of the neutral excited states with respect to the neutral ground state using MRCI + SO to include the SO coupling effects, as shown in Table 1. For BiB_2O, the two calculated ΔE term values are in excellent agreement with the observed values from bands A and B. The X and A bands are due to SO splitting of the $^2\Pi$ state ($^2\Pi_{3/2}$ and $^2\Pi_{1/2}$) from removal of an electron from the 2π HOMO, which explains why these two bands have similar intensities and identical vibrational structures (Figure 1). The calculated SO splitting of 0.54 eV is in excellent agreement with the experimental value of 0.56 eV, which is large enough to quench the Renner–Teller effect so that the neutral linear BiB_2O does not undergo bending distortions.[27] Band B at 5.35 eV corresponds to the removal of an electron from the 5σ HOMO−1, which is mainly a nonbonding MO (Supporting Information, Figure S1). For Bi_2B, two different reference states were employed to compute the ΔE term values according to their different electronic natures. The SOMOs ($1\pi_g$) are basically degenerate nonbonding MOs consisting of Bi 6p orbitals (Supporting Information, Figure S1b). The removal of one electron from the $1\pi_g$ orbital results in the $^2\Pi_g$ final state, which gives rise to two SO-coupled states, $^2\Pi_{g1/2}$ and $^2\Pi_{g3/2}$. The calculated splitting of these two states is 1.02 eV, indicating that the $^2\Pi_{g3/2}$ state may account for the observed bands C or D. Again, the Renner–Teller effect can be quenched by such a large spin–orbit splitting to avoid bending distortion in the linear neutral Bi_2B.[27] All the other excited states result from the removal of an electron from the deeper fully occupied MOs with two unpaired electrons in the $1\pi_g$ orbitals, resulting in both doublet and quartet excited states for the neutral. Thus, the ΔE term values of these excited states were calculated with respect to the lowest quartet state, corresponding to band A. As expected, very complicated electronic states are derived because of the unpaired electrons and the SO coupling. Overall, the theoretical calculations allow the PE spectra to be qualitatively understood, as shown in Table 1.

Apart from the MO analyses, we also performed bonding analyses for BiB_2O^- and Bi_2B^- using the adaptive natural density partitioning (AdNDP) method at the PBE0/AVTZ level,[28] as shown in Figure 4. The AdNDP analysis for BiB_2O^- clearly identifies a Bi 6s and an O sp lone pair, a Bi≡B triple bond, a B−B single bond, and a B≡O triple bond (Figure 4a). Thus, the structures of BiB_2O^- can be expressed as $[Bi{\equiv}B{-}B{\equiv}O]^-$, which is an electron-precise molecule and underscores its high stability. The BiB_2O^- species is the first molecule to be observed experimentally to contain a Bi≡B triple bond. A valent isoelectronic NB_2O^- species was observed previously in a low-temperature matrix.[29] However, a $[B{\equiv}N{-}B{\equiv}O]^-$ Lewis structure was assigned on the basis of infrared spectroscopy. It is possible that the more electronegative N atom disfavors the terminal position, although a $[N{\equiv}B{-}B{\equiv}O]^-$ Lewis structure would fulfill the octet rule better. The AdNDP analysis for Bi_2B^- reveals two 2c–1e bonds on Bi (essentially nonbonding 6p electrons), two 6s lone pairs, two Bi−B σ bonds, and two 3c–2e Bi−B−Bi π bonds. Hence, the bonding in Bi_2B^- can be described as two Bi=B double bonds, that is, $[Bi{=}B{=}Bi]^-$, which is paramagnetic. The Bi_2B^- species is the first molecule to feature a Bi=B double bond. Together with the Bi−B single bond observed in Bi-B≡O$^-$ previously,[10] we now have the full range of bonds between boron and bismuth. The calculated Bi−B single, double, and triple bond lengths in $BiBO^-$, Bi_2B^-, and BiB_2O^- at the PBE0/AVTZ level are 2.256 Å, 2.138 Å, and 2.036 Å, respectively. These bond lengths compare favorably with those obtained from Pyykko's self-consistent atomic covalent radii,[30] that is, 2.36 Å, 2.19 Å, and 2.08 Å, for Bi−B, Bi=B, and Bi≡B, respectively. We also evaluated the Bi−B triple, double, and single bond strengths by the following equations: $BiB_2O^- \rightarrow Bi + B_2O^-$ (4.70 eV), $Bi_2B^- \rightarrow Bi + BBi^-$ (3.21 eV), and $BiBO^- \rightarrow Bi + BO^-$ (2.34 eV) at the PBE0/AVTZ level. We see a good correlation between the bond lengths/bond orders and the bond strengths. The B−Bi multiple bonds in BiB_2O^- and Bi_2B^- are reminiscent of the well-known B−N multiple bonds in the $[L_nM{-}B{\equiv}N{-}R]$ and $[(CO)_5M{=}B{=}N(SiME_3)_2]$ compounds.[31] Even though the B−Bi multiple bonds are slightly weaker than their B−N counterparts, the current study suggests the possibility of synthesizing chemical compounds with bismuth–boron multiple bonds and other boron–metal triple bonds.

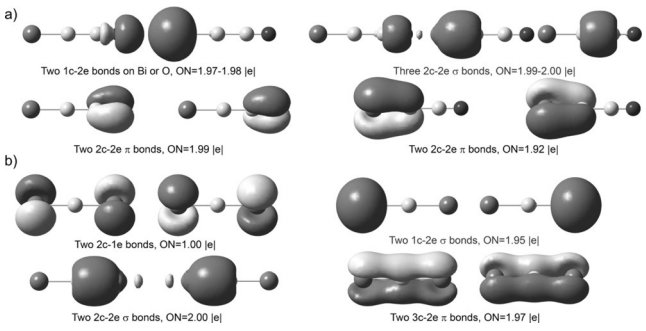

Figure 4. Chemical bonding analyses using AdNDP for a) BiB_2O^- and b) Bi_2B^- at the PBE0/AVTZ level.

Acknowledgements

This work was supported by the National Science Foundation (CHE-1263745). The calculations were performed using resources at the Center for Computation and Visualization (CCV) of Brown University. T.J. wishes to thank the Chemistry Department of Brown University for the Vince Wernig Fellowship.

Conflict of interest

The authors declare no conflict of interest.

Keywords: ab initio calculations · bismuth · boron · multiple bonds · photoelectron spectroscopy

How to cite: *Angew. Chem. Int. Ed.* **2017**, *56*, 9551 – 9555
Angew. Chem. **2017**, *129*, 9679 – 9683

[1] W. N. Lipscomb, *Science* **1977**, *196*, 1047 – 1055.
[2] a) L. S. Wang, *Int. Rev. Phys. Chem.* **2016**, *35*, 69 – 142; b) A. I. Boldyrev, L. S. Wang, *Phys. Chem. Chem. Phys.* **2016**, *18*, 11589 – 11605; c) A. P. Sergeeva, I. A. Popov, Z. A. Piazza, W. L. Li, C. Romanescu, L. S. Wang, A. I. Boldyrev, *Acc. Chem. Res.* **2014**, *47*, 1349 – 1358; d) A. N. Alexandrova, A. I. Boldyrev, H. J. Zhai, L. S. Wang, *Coord. Chem. Rev.* **2006**, *250*, 2811 – 2866.
[3] M. Zhou, N. Tsumori, Z. Li, K. Fan, L. Andrews, Q. Xu, *J. Am. Chem. Soc.* **2002**, *124*, 12936 – 12937.
[4] S. D. Li, H. J. Zhai, L. S. Wang, *J. Am. Chem. Soc.* **2008**, *130*, 2573 – 2579.
[5] L. C. Ducati, N. Takagi, G. Frenking, *J. Phys. Chem. A* **2009**, *113*, 11693 – 11698.
[6] H. Braunschweig, R. D. Dewhurst, K. Hammond, J. Mies, K. Radacki, A. Vargas, *Science* **2012**, *336*, 1420 – 1422.
[7] H. J. Zhai, L. M. Wang, S. D. Li, L. S. Wang, *J. Phys. Chem. A* **2007**, *111*, 1030 – 1035.
[8] a) H. J. Zhai, S. D. Li, L. S. Wang, *J. Am. Chem. Soc.* **2007**, *129*, 9254 – 9255; b) H. J. Zhai, C. Q. Miao, S. D. Li, L. S. Wang, *J. Phys. Chem. A* **2010**, *114*, 12155 – 12161; c) H. J. Zhai, J. C. Guo, S. D. Li, L. S. Wang, *ChemPhysChem* **2011**, *12*, 2549 – 2553; d) Q. Chen, H. J. Zhai, S. D. Li, L. S. Wang, *J. Chem. Phys.* **2012**, *137*, 044307; e) H. Bai, H. J. Zhai, S. D. Li, L. S. Wang, *Phys. Chem. Chem. Phys.* **2013**, *15*, 9646 – 9653; f) Q. Chen, H. Bai, H. J. Zhai, S. D. Li, L. S. Wang, *J. Chem. Phys.* **2013**, *139*, 044308; g) H. J. Zhai, Q. Chen, H. Bai, H. G. Lu, W. L. Li, S. D. Li, L. S. Wang, *J. Chem. Phys.* **2013**, *139*, 174301; h) H. J. Zhai, Q. Chen, H. Bai, S. D. Li, L. S. Wang, *Acc. Chem. Res.* **2014**, *47*, 2435 – 2445.
[9] D. Y. Zubarev, A. I. Boldyrev, J. Li, H. J. Zhai, L. S. Wang, *J. Phys. Chem. A* **2007**, *111*, 1648 – 1658.
[10] T. Jian, G. V. Lopez, L. S. Wang, *J. Phys. Chem. B* **2016**, *120*, 1635 – 1640.
[11] H. Braunschweig, K. Radacki, A. Schneider, *Science* **2010**, *328*, 345 – 347.
[12] a) C. Romanescu, T. R. Galeev, W. L. Li, A. I. Boldyrev, L. S. Wang, *Acc. Chem. Res.* **2013**, *46*, 350 – 358; b) I. A. Popov, T. Jian, G. V. Lopez, A. I. Boldyrev, L. S. Wang, *Nat. Commun.* **2015**, *6*, 8654; c) T. Jian, W. L. Li, X. Chen, T. T. Chen, G. V. Lopez, J. Li, L. S. Wang, *Chem. Sci.* **2016**, *7*, 7020 – 7027; d) W. L. Li, T. Jian, X. Chen, H. R. Li, T. T. Chen, X. M. Luo, S. D. Li, J. Li, L. S. Wang, *Chem. Commun.* **2017**, *53*, 1587 – 1590.
[13] X. Wang, B. O. Roos, L. Andrews, *Angew. Chem. Int. Ed.* **2010**, *49*, 157 – 160; *Angew. Chem.* **2010**, *122*, 161 – 164.
[14] a) H. Braunschweig, M. Colling, *Coord. Chem. Rev.* **2001**, *223*, 1 – 51; b) H. Braunschweig, C. Kollann, D. Rais, *Angew. Chem. Int. Ed.* **2006**, *45*, 5254 – 5274; *Angew. Chem.* **2006**, *118*, 5380 – 5400; c) D. Vidovic, G. A. Pierce, S. Aldridge, *Chem. Commun.* **2009**, 1157 – 1171.
[15] H. Braunschweig, K. Radacki, D. Rais, F. Seeler, *Angew. Chem. Int. Ed.* **2006**, *45*, 1066 – 1069; *Angew. Chem.* **2006**, *118*, 1087 – 1090.
[16] J. S. Lu, S. H. Su, M. C. Yang, X. T. Wen, J. Z. Xie, M. D. Su, *Organometallics* **2016**, *35*, 3924 – 3931.
[17] J. Moon, J. S. Lim, J. Kim, *Int. J. Quantum Chem.* **2017**, *117*, e25324, https://doi.org/10.1002/qua.25324.
[18] L. S. Wang, H. S. Cheng, J. Fan, *J. Chem. Phys.* **1995**, *102*, 9480 – 9493.
[19] a) C. Adamo, V. Barone, *J. Chem. Phys.* **1999**, *110*, 6158 – 6170; b) G. D. Purvis III, R. J. Bartlett, *J. Chem. Phys.* **1982**, *76*, 1910 – 1918; c) G. E. Scuseria, C. L. Janssen, H. F. Schaefer III, *J. Chem. Phys.* **1988**, *89*, 7382 – 7387.
[20] H. J. Werner, P. J. Knowles, *J. Chem. Phys.* **1985**, *82*, 5053 – 5063.
[21] H. J. Werner, P. J. Knowles, *J. Chem. Phys.* **1988**, *89*, 5803 – 5814.
[22] A. Berning, M. Schweizer, H. J. Werner, P. J. Knowles, P. Palmieri, *Mol. Phys.* **2000**, *98*, 1823 – 1833.
[23] K. A. Peterson, *J. Chem. Phys.* **2003**, *119*, 11099 – 11112.
[24] R. A. Kendall, T. H. Dunning, Jr., R. J. Harrison, *J. Chem. Phys.* **1992**, *96*, 6796 – 6806.
[25] M. J. Frisch, G. W. Trucks, H. B. Schlegel, G. E. Scuseria, M. A. Robb, J. R. Cheeseman, G. Scalmani, V. Barone, B. Mennucci, G. A. Petersson, H. Nakatsuji, M. Caricato, X. Li, H. P. Hratchian, A. F. Izmaylov, J. Bloino, G. Zheng, J. L. Sonnenberg, M. Hada, M. Ehara, K. Toyota, R. Fukuda, J. Hasegawa, M. Ishida, T. Nakajima, Y. Honda, O. Kitao, H. Nakai, T. Vreven, J. A. Montgomery, Jr., J. E. Peralta, F. Ogliaro, M. J. Bearpark, J. Heyd, E. N. Brothers, K. N. Kudin, V. N. Staroverov, R. Kobayashi, J. Normand, K. Raghavachari, A. P. Rendell, J. C. Burant, S. S. Iyengar, J. Tomasi, M. Cossi, N. Rega, N. J. Millam, M. Klene, J. E. Knox, J. B. Cross, V. Bakken, C. Adamo, J. Jaramillo, R. Gomperts, R. E. Stratmann, O. Yazyev, A. J. Austin, R. Cammi, C. Pomelli, J. W. Ochterski, R. L. Martin, K. Morokuma, V. G. Zakrzewski, G. A. Voth, P. Salvador, J. J. Dannenberg, S. Dapprich, A. D. Daniels, Ö. Farkas, J. B. Foresman, J. V. Ortiz, J. Cioslowski, D. J. Fox, Gaussian, Inc., Wallingford, CT, USA, **2009**.
[26] H. Werner, P. Knowles, R. Lindh, F. Manby, M. Schütz, P. Celani, T. Korona, G. Rauhut, R. Amos, A. Bernhardsson, *MOLPRO* **2012**.
[27] a) R. Renner, *Z. Phys.* **1934**, *92*, 172 – 193; b) Y. L. Wang, H. J. Zhai, L. Xu, J. Li, L. S. Wang, *J. Phys. Chem. A* **2010**, *114*, 1247 – 1254.
[28] D. Y. Zubarev, A. I. Boldyrev, *Phys. Chem. Chem. Phys.* **2008**, *10*, 5207 – 5217.
[29] M. F. Zhou, N. Tsumori, Q. Xu, G. P. Kushto, L. Andrews, *J. Am. Chem. Soc.* **2003**, *125*, 11371 – 11378.
[30] P. Pyykkö, *J. Phys. Chem. A* **2015**, *119*, 2326 – 2337.
[31] a) H. Braunschweig, K. Radacki, D. Rais, K. Uttinger, *Angew. Chem. Int. Ed.* **2006**, *45*, 162 – 165; *Angew. Chem.* **2006**, *118*, 169 – 172; b) H. Braunschweig, *Angew. Chem. Int. Ed.* **1998**, *37*, 1786 – 1801; *Angew. Chem.* **1998**, *110*, 1882 – 1898.

Manuscript received: May 19, 2017
Accepted manuscript online: June 14, 2017
Version of record online: June 30, 2017

